Ding, K.R., Luo, J.F., Di, H.J., Clough, T., Ledgard, S., Lindsey, S. 2023. THE EFFECTS OF DIFFERENT COW URINARY NITROGEN RATES ON GASEOUS NITROGEN FLUXES FROM PASTURE SOIL. In: Diverse Solutions for Efficient Land, Water and Nutrient use. (Eds. C.L. Christensen, D.J. Horne and R. Singh). http://flrc.massey.ac.nz/publications.html. Occasional Report No. 35. Farmed Landscapes Research Centre, Massey University, Palmerston North, New Zealand. 18 pages.

THE EFFECTS OF DIFFERENT COW URINARY NITROGEN RATES ON GASEOUS NITROGEN FLUXES FROM PASTURE SOIL

Keren Ding[1,2], Jiafa Luo[1], Hongjie Di[2], Timothy Clough[2], Stewart Ledgard[1], Stuart Lindsey[1]

[1]*Ruakura Research Centre, 10 Bisley Road, Hamilton 3214, New Zealand*
[2]*Soil & Physical Sciences Department, Lincoln University, Christchurch, New Zealand*
Email: keren.ding@agresearch.co.nz

Abstract

Cattle grazing pasture deposit urine at high nitrogen (N) rates that can impact the environment. Among the loss pathways, denitrification, which produces nitrous oxide (N_2O) and dinitrogen (N_2), is a major way that N can be lost to the atmosphere. There is limited information about N_2 losses from grazed-pasture systems after urine deposition due to the method limitations with high ambient N_2 concentrations. In this study, the ^{15}N flux method and a high sampling frequency were used to explore N_2 and N_2O fluxes over time after urine application at two rates (400 and 800 kg N ha^{-1}) on a New Zealand grazed pasture soil. N_2O fluxes were significantly higher from the higher N application rate compared with the lower rate but there was no significant difference in N_2 fluxes. Dinitrogen was the predominant gaseous N form lost from the applied urinary-N, contributing 32.1 ± 4.1% and 14.4 ± 1.7% of the total deposited N from 400 kg N ha^{-1} and 800 kg N ha^{-1}, respectively, over the 95 measurement days. Denitrification and codenitrification both occurred in the pasture system, with denitrification being the predominant N_2 production pathway, contributing 97.9 – 98.5% of the total N_2 production. The similar N_2 losses between the two urine-N rates is speculated to be due to enhanced ammonia volatilisation and transfer of N as nitrate, to deeper soil layers at the higher N rate. Soil relative gas diffusivity indicated that high N_2 fluxes may have resulted from entrapped N_2 diffusing from the draining soil.

Keywords: Denitrification, Urine patch, N cycling, N_2O, N_2, ^{15}N

Introduction

Ruminant urine excreted onto pasture soils generates soil inorganic nitrogen (N) concentrations that exceed the pasture's immediate demand (Selbie et al., 2015a). Consequently, surplus N may be lost from the pasture via nitrate (NO_3^-) leaching, ammonia (NH_3) volatilization, and other gaseous N emissions that include nitrous oxide (N_2O), nitric oxide (NO), and dinitrogen (N_2) (Khan et al., 2011; Friedl et al., 2017; Luo and Ledgard, 2020). Of these losses, only N_2 is environmentally benign. Nitrous oxide is a potent greenhouse gas with a global warming potential 273 times that of carbon dioxide (CO_2) over a 100-year time period (IPCC, 2022), and it is also the dominant ozone depleting substance (Ravishankara et al., 2009). In grazed

pasture systems, ruminant urine patches are sites of high N_2O emissions (Selbie et al., 2015a). In pasture soils, multiple pathways produce N_2O, including denitrification, nitrifier-denitrification, nitrification, and dissimilatory nitrate reduction to ammonium (DNRA) (Butterbach-Bahl et al., 2013). The only sink for N_2O in soils is its conversion to N_2. This may occur via the denitrification pathway, where denitrifiers contain the nosZI gene, or via nondenitrifying microbes that contain the nosZII gene (Hallin et al., 2018; Shan et al., 2021).

Urinary-N loading rates in the urine patch can vary from 200-2000 kg N ha^{-1} due to different urinary N concentrations, urination frequencies, and urine volumes (Selbie et al., 2015a). The Intergovernmental Panel on Climate Change (IPCC) global default urine-derived N_2O emission factor (EF_3, the percentage of urinary N lost as N_2O) is 0.4% (IPCC, 2019), however, this EF_3 value can vary as a result of differing climatic and environmental factors (Singh et al., 2021). This is likely the result of both N_2O production and consumption occurring simultaneously. These processes may be affected independently by the spatial and temporal interactions between the soil microbiome and the soil's physical and chemical characteristics (Morales et al., 2015; Samad et al., 2016; Highton et al., 2020; Ganasamurthy et al., 2021). Soil moisture also plays a key role in regulating N_2O production and consumption since it affects soil aeration (Friedl et al., 2016) and it is the level of soil aeration which determines the potential for denitrification to occur: the denitrification process requires anaerobic conditions for N_2O consumption and the production of N_2. Relative soil gas diffusivity (Dp/Do), which is the ratio of the soil-gas diffusion coefficient to the free-air gas diffusion coefficient, is a metric that can be used for understanding the functional pore space for oxygen to diffuse into a soil. The onset of anaerobic conditions has been shown to commence when the soil Dp/Do is ≤ 0.02 (Stepniewski, 1980). Balaine et al. (2016) found that production of N_2O in repacked soil cores increased as Dp/Do declined below ≤ 0.02, with significant N_2 production when Dp/Do was < 0.006.

Due to method limitations, that include the existence of a relatively high background N_2 concentration in air, *in situ* data on N_2 flux dynamics following ruminant urine deposition, and the factors affecting the N_2O consumption pathway, are scarce (Selbie et al., 2015b; Clough et al., 2017; Friedl et al., 2017). After applying ^{15}N labelled urine (1000 kg N ha^{-1}) to a pasture in Ireland, Selbie et al. (2015b) found N_2 fluxes dominated (98.9%) the gaseous loss of N (N_2O+N_2), with codenitrification being a major N_2 production pathway in a pasture soil. Codenitrification is a co-metabolism pathway that forms hybrid N_2 and N_2O by combining one N atom from nitrite (NO_2^-) or nitric oxide (NO) and another N atom from a co-metabolised compound such as NH_3, hydrazine (N_2H_4), amino compounds, or hydroxylamine (Spott et al., 2011). The limited number of studies to date means that the significance of N_2 fluxes as a N loss pathway from grazed pasture systems remains unresolved.

Therefore, the aims of this *in situ* study were: 1) to measure the N_2 fluxes and N_2O fluxes over time in a grazed pasture following synthetic urine application at two different rates (400 and 800 kg N ha^{-1}); 2) to explore the N_2 production pathways in a grazed pasture soil.

Methods and Materials

Study site

The field experiment was conducted on an established ryegrass (*Lolium perenne* L.)/white clover (*Trifolium repens*) pasture in the Waikato region of New Zealand (37°46'S, 175°18'E). The soil was a Te Kowhai silt loam soil, a Typic Orthic Gley Soil (NZ soil classification, (Hewitt, 1993)) or Typic Ochraqualf (U.S.A soil taxonomy, (Soil Survey Staff, 1975)). The soil is halloysitic and poorly drained with a slowly permeable subsoil (Dominati et al., 2016).

The basic soil properties of the experimental soil are shown in Table 1. The Waikato region has a temperate climate with a mean 1240 mm annual rainfall and a mean annual air temperature of 14°C.

Table 1 Properties of the experimental soil (0-7.5 cm).

soil type	pH	Olsen P (mg L^{-1})	CEC (me 100 g^{-1})	Total N (g kg^{-1})	$C_{organic}$ (g kg^{-1})	Bulk density (g cm^{-3})
Te Kowhai	5.8	21	23	7.7	72	0.85

Experimental setup

Three treatments included: a control with no N addition (CK), and synthetic urinary-N applied at either 400 kg N ha^{-1} (U400) or 800 kg N ha^{-1} (U800). A complete randomised block design was used, with 4 replicate plots (73 cm × 73 cm) and 6 replicate chambers (24 cm internal diameter with a height of 10 cm) for each treatment. The 95-day experimental period commenced with treatment application on 21st August 2020 (Day 0), late winter, and ended on 23rd November 2020, late spring.

Synthetic urine (hereafter called urine) was prepared according to Kool et al. (2006a). It constituted 85.2% urea-N, 4.1% hippuric acid-N, 8.3% allantoin-N and 2% creatinine-N. To mimic real urine, the urine solution contained 14 g L^{-1} $KHCO_3$, 10.5 g L^{-1} KCl, 0.3 g L^{-1} $CaCl_2$, 1.32 g L^{-1} $MgCl_2 \cdot 6H_2O$ and 3.7 g L^{-1} Na_2SO_4. The total N contents of the urine were 4 g N L^{-1} and 8 g N L^{-1} in the U400 and U800 treatments, respectively, and 5.33 L and 0.45 L were applied to the plots and chambers, respectively, at a rate equivalent to 10 L m^{-2} (Haynes and Williams, 1993).

Gas sampling and analysis

A non-steady state chamber method was used for measuring N_2O and N_2 fluxes from the field. Measurements were taken daily for the first month after urine application, and then three times a week for the second month, and once a week in the third month with extra samplings conducted when rainfall exceeded 10 mm in 24 hours (de Klein et al., 2014). Sampling ceased when soil properties and gas fluxes within the U400 and U800 treatments equalled those of the CK treatment. Headspace gas samples (15 mL) were taken at 0, 20 and 40 min after chamber enclosure, using a syringe fitted with a 0.5 mm by 16 mm needle, and transferred into pre-evacuated 6 mL septum-sealed screw-capped glass vials (Exetainer, Labco Ltd, High Wycombe, UK). Gas samples for N_2O-^{15}N enrichment and N_2 flux measurement were taken after 3 hours from the chamber enclosure using a 15-mL glass syringe fitted with a 3-way tap and a 0.5 mm by 16 mm needle. The gas samples were placed in pre-evacuated 12 mL vials (Exetainer, Labco Ltd, High Wycombe, UK). An automated gas chromatograph (8610; SRI Instruments, Torrance, CA), coupled to an autosampler (Gilson 222XL; Gilson, Middleton, WI), was used to determine N_2O gas concentrations in the samples (Clough et al., 2006). A continuous-flow-isotope mass spectrometer (Sercon 20/20; Secron, Chesire, UK) inter-faced with a TGII cryofocusing unit (Sercon, Chesire, UK), was used to determine the ion currents 44, 45 and 46 for N_2O and 28, 29 and 30 for N_2 with the ^{15}N enrichment of the N_2O-N and N_2-N gas samples determined according to Stevens et al. (1993).

The N_2O fluxes (mg N m^{-2} day^{-1}) were calculated from the increase in headspace N_2O over the sampling period (Singh et al., 2021):

$$F_{N_2O} = b \times \frac{V}{A} \times \frac{M}{Vcorr} \times 1440 \div 1000$$

Where, F_{N2O} is the N_2O flux (mg N m^{-2} day^{-1}); *b* is the increase in N_2O concentration per min enclosure period (μL L^{-1} min^{-1}); V is the headspace volume of the chamber (L); A is the basal area of the chamber (m^2); M is the molecular weight of N_2O-N (28 g mol^{-1}). The constants 1440 and 1000 are the conversion factors for minutes (min) to one day, and micrograms (μg) to one milligram (mg), respectively.

$$\text{Vcorr} = 22.4 \times (\frac{273.15+T}{273.15})$$

where, V_{corr} (L mol^{-1}) is as defined; T is headspace air temperature (°C) in the chamber during the measurements; 22.4 L is the molar volume of an ideal gas at 1-atm, 273.15 °(Aylward and Findlay, 1973).

Cumulative N_2O emissions, over 95 days, were calculated using linear interpolation between sampling events. The N_2O EF_3 value (N_2O-N emitted as a % of N applied) was then calculated by dividing the treatment-induced cumulative emission by the amount of N applied for a given treatment (de Klein et al., 2014):

$$EF_3 = \frac{\text{Urine } N_2O - \text{Control } N_2O}{\text{Urine N applied}} \times 100$$

Where EF_3 is the urine emission factor (N_2O-N emitted as a % of N applied), urine N_2O and control N_2O are the cumulative N_2O emissions from urine and control plots, respectively (kg N ha^{-1}) and urine N applied is the rate of N applied (kg N ha^{-1}).

The ^{15}N flux method

For N_2O, the mass (*m*)/charge(*z*) ratios derived from the ion currents (I) 44, 45 and 46 enabled concentrations and molecular ratios ^{45}R ($^{45}I/^{44}I$) and ^{46}R ($^{46}I/^{44}I$) to be calculated. The sources of N_2O were then apportioned into the fraction (d'_D) derived from the denitrifying pool of enrichment a_D and the fraction $d'_N = (1\text{-}d'_D)$ derived from the pool or pools at natural abundance (Stevens et al., 1993; Arah, 1997).

For N_2, the ion currents at *m/z* 28, 29 and 30 enabled molecular ratios ^{29}R ($^{29}I/^{28}I$) and ^{30}R ($^{30}I/^{28}I$) to be determined. Differences between the molecular ratios of enriched and ambient atmospheres were expressed as $\Delta^{29}R$ and $\Delta^{30}R$. Then the flux of N_2 was calculated using three different methods (Selbie et al., 2015b):

1) the enrichment of the denitrifying pool ($^{15}X_N$) was calculated using $\Delta^{29}R$ and $\Delta^{30}R$ and the N_2 flux (Mulvaney and Boast, 1986);
2) using the equation of Mulvaney (1984) and the $\Delta^{30}R$ data, with the assumption that the enrichment of the denitrifying pool was a_D (Stevens and Laughlin, 2001); and
3) using $\Delta^{29}R$ and $\Delta^{30}R$ to calculate the relative contributions of true denitrification (N_{2true}), according to method 2, and Codenitrification (N_{2CO}).

Increases in $\Delta^{29}R$ and $\Delta^{30}R$ may occur from true denitrification (hereafter called denitrification), but codenitrification contributes most to $\Delta^{29}R$ where the ratio of $\Delta^{29}R$ to $\Delta^{30}R$ is always 272 (Clough et al., 2001). By assuming all $\Delta^{30}R$ was the result of denitrification, method 2, N_{2true} was calculated. According to Clough et al. (2001), the fraction of the total number of moles of N_2 in the headspace, resulting from codenitrification (d_{CO}) was calculated as follows:

$$d_{CO} = -\Delta^{29}Rp_1^2 / (-\Delta^{29}Rp_1^2 + \Delta^{29}Rp_1p_2 + q_1p_2 - q_2p_1)$$

where p_1 (0.9963) and q_1 (0.0037) represent the atom fractions of ^{14}N and ^{15}N in the natural abundance pool, respectively, p_2 and q_2 are the atom fractions of ^{14}N and ^{15}N in the enriched nitrate pool from which codenitrification is assumed to occur. The N_2 fluxes from denitrification and codenitrification were calculated according to the equation from (Mulvaney and Boast, 1986). The N_2 fluxes were set to 0 if $\Delta^{29}R < 1.6 \times 10^{-6}$ or $\Delta^{30}R < 2.0 \times 10^{-7}$.

Soil sampling and analysis

Daily precipitation data were collected from the weather station located at the field site. Soil variables were sampled, twice per week, by taking two soil cores (7.5 cm long, 2.5 cm diameter) from each of the 12 plots. Immediately after sampling, the holes were backfilled with solid PVC tubes (2.5 cm diameter). Soil samples were sieved through 4 mm mesh and then extracted with 0.5 M K_2SO_4 (ratio 1:5 dry soil: K_2SO_4) for 2 h (Jones and Willett, 2006). Soil extractions were filtered through Whatman No. 42 filter paper, and filtrates were frozen until analysis for NO_3^--N, NO_2^--N, and ammonium (NH_4^+-N), using a Skalar SAN^{++} segmented flow analyser (Skalar Analytical B.V., Breda, Netherlands), and extractable organic carbon (EOC) using a TOC analyser (Shimadzu, Japan). Soil pH was measured using a standard electrode (Mettler Toledo, Switzerland) in 1:2.5 (w/v) soil-distilled water suspensions (Blakemore et al., 1987). Soil gravimetric moisture content was determined after drying at 105°C for 24 h. Soil temperature (5 cm depth) and air temperature were measured using a digital thermometer on each sampling day.

Soil water-filled pore space (WFPS) (%) was calculated as:

$$\text{WFPS} = \frac{GSMC \times BD}{1-\frac{\text{BD}}{\text{PD}}} \times 100$$

where GSMC is the gravimetric soil moisture content, PD is the particle density (2.65 g cm^{-3}), BD is the soil bulk density.

Relative gas diffusivity (Dp/Do) was calculated according to Moldrup et al. (2013) as:

$$\frac{D_p}{D_o} = \varepsilon^{[1+C_m\Phi]}\left(\frac{\varepsilon}{\Phi}\right)$$

where ε is the air-filled porosity (m^3 soil air m^{-3} soil), ϕ is the soil total porosity (m^3 pore space m^{-3} soil), and C_m is the recommended structure-dependent water-induced linear reduction parameter value for intact soils which was set to a value of 2.1 as recommended by Moldrup et al. (2013) for intact soils.

^{15}N recovery in the plant and soil pools

During the experimental period (95 days), the pasture was harvested four times, on days 20, 42, 68, and 94. Harvested above-ground material was oven-dried at 60°C, ground with a planetary cylinder mill, and analysed for ^{15}N enrichment using an IRMS. At the end of the experiment, soil cores (0–45 cm) were collected from within the chambers and divided into 4 different layers (0–7.5 cm, 7.5–15 cm, 15–30 cm, 30–45 cm). These were air-dried, and roots and plant litter were removed before samples were milled and analysed for total N content and ^{15}N enrichment using IRMS. Recoveries of ^{15}N for soil and pasture were calculated according to Zapata (2001). Variance of the total ^{15}N recovered, from the measured ^{15}N pools, was determined by summing the variances of individual ^{15}N pools along with twice the covariance of all the possible two-way combinations of these pools (Snedecor and Cochran, 1967; Legg and Meisinger, 1982).

Statistical analysis

Statistical analyses were conducted using R4.0.5 (R Development Core Team, 2021). The normality and homoscedasticity of variance of all variables were tested by diagnostic plots as Histogram and QQ plots. The N_2O fluxes, NH_4^+ and NO_3^- concentrations showed a skewed distribution and required natural log-transformation prior to statistical analysis. Measured variables were tested for outliers using the box-plot method and removed if detected, < 5% of data were removed for each variable (Schwertman et al., 2004). The effects of treatments on soil properties, gas fluxes and ^{15}N recovery rates were analysed using a mixed effects model (Time * Treatments+(1|plot)) where treatments, time and their interaction were fixed effects and where plot was the random effect. Tukey-HSD test ($P<0.05$) was chosen to perform pair-wise comparison in the model. The above analyses were conducted using packages 'lme4' (Bates et al., 2014) and 'predictmeans' (Luo et al., 2018). Figures were produced using SigmaPlot 14.0.

Results

Rainfall, soil temperature, moisture and diffusivity

Total precipitation over the experimental period equalled 198 mm with individual daily rainfall events ranging from 0.3 to 23.4 mm (Figure 1a). Heavy rainfall (> 10 mm) occurred on 5 occasions: day 17, 37, 53, 76 and 79 (Figure 1a). The daily soil temperature (5 cm soil depth) trended upward over time, from 12℃ in August to 19℃ in November 2020 (Figure 1a). Generally, Dp/Do was < 0.02 from day 0 to day 87 and < 0.006 for the majority of the experimental period except days 45 to 52, 62 to 73 and 87 to 94 (Figure 1b). Soil water-filled pore space (WFPS) over the 0-7.5 cm depth fluctuated between 60% and 84% for almost the entire experimental period, the exception being day 94 where it was ~ 50% (Figure 1c).

Soil mineral N (0-7.5 cm)

Soil NH_4^+-N concentrations in the 0-7.5 cm soil depth (Figure 2a) following urine deposition were higher ($P<0.001$) than in the CK treatment. The general temporal pattern in urine-treated soil was for the NH_4^+-N concentration to increase immediately after urine addition and then decline to a level observed in the CK treatment, which occurred at day 25 and day 42 in the U400 and U800 treatments, respectively (Figure 2a). In the U400 and U800 treatments the peak of NH_4^+-N concentrations occurred on days 4 and 11, with respective values of 312 ± 12 mg N kg^{-1} soil and 487 ± 76 mg N kg^{-1} soil. Soil NO_2^--N concentrations never exceeded 1 mg N kg^{-1} soil and remained unaffected by urine deposition (data not shown).

Urine addition increased ($P<0.001$) soil NO_3^--N concentrations in the 0-7.5 cm depth with concentrations increasing to 78 ± 21 mg N kg^{-1} soil (day 25) and 178 ± 33 mg N kg^{-1} (day 35) in the U400 and U800 treatments, respectively (Figure 2b). In the U400 treatment the soil NO_3^--N concentration had declined to equal that of the CK treatment by day 54, however, in the U800 treatment soil NO_3^--N concentrations remained elevated until the end of the experiment (Figure 2b).

Following urine addition, the soil pH, averaged over the 0-7.5 cm depth, initially increased ($P<0.05$) from 5.5 ± 0.1 in the CK treatment to 6.1 ± 0.1 and 6.3 ± 0.2, in the U400 and U800 treatments, respectively (Figure 3). The soil pH values then decreased in both urine treatments. However, in the U800 treatment the rate of decrease was slower, and it took longer for the pH

to return to that observed in the CK treatment (Figure 3). The soil pH in the U800 treatment was lower than that observed in the CK treatment from days 25 to 56 (Figure 3).

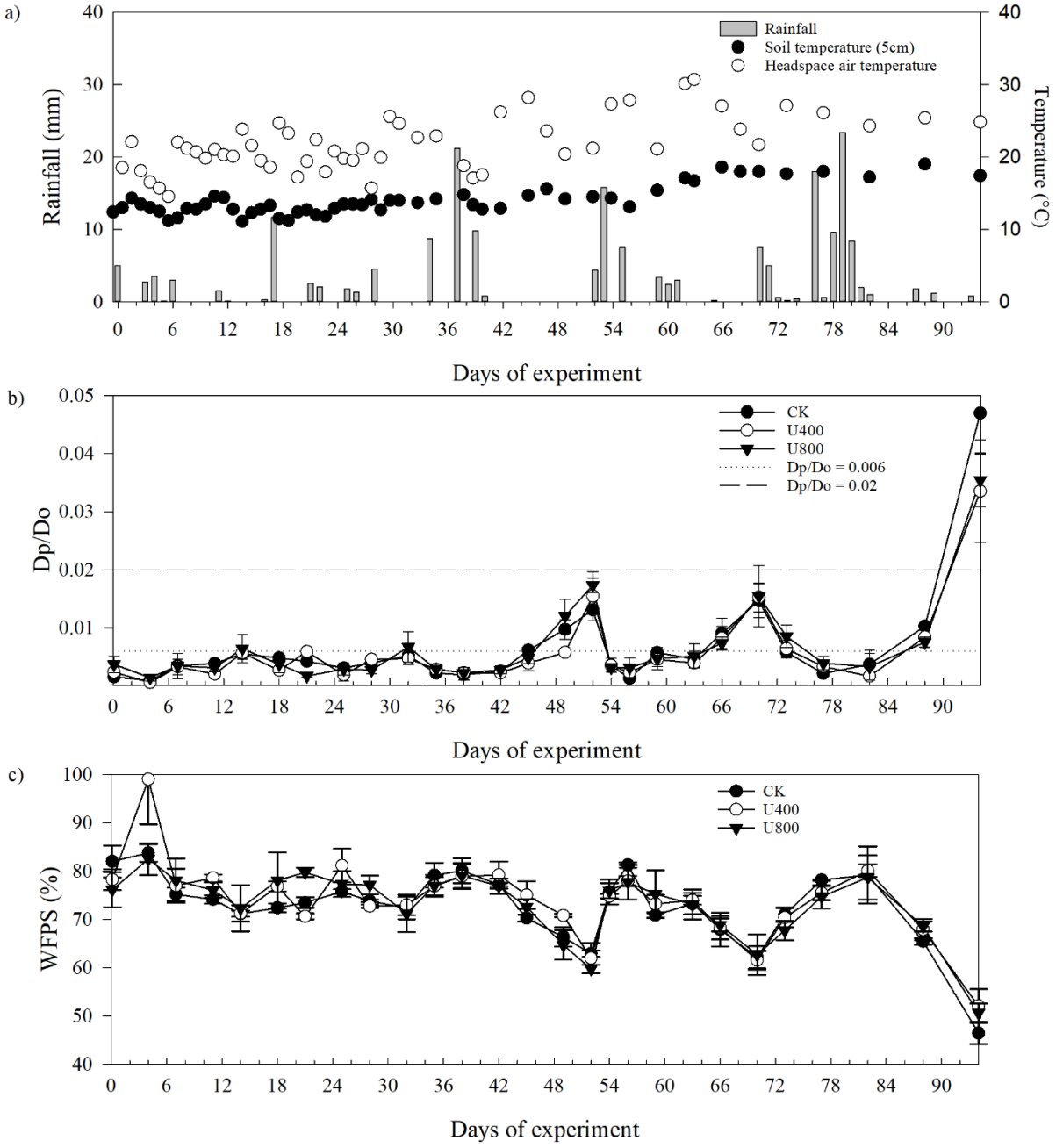

Figure 1. Temporal changes in daily soil temperature (5 cm depth), headspace air temperature (ºC), and daily rainfall (mm) (a), soil relative gas diffusivity (Dp/Do) (0-7.5 cm depth) (b), soil water-filled pore space (WFPS) (0-7.5 cm depth) (c). Symbols are means (*n* = 4) with vertical error bars the standard error of the mean. The dashed line in (b) is the proposed threshold (Dp/Do = 0.02) for the formation of anaerobic sites in the soil matrix (Stepniewski, 1980) and the dotted line is the observed threshold (Dp/Do = 0.006) for increased production of N_2 (Balaine et al., 2016)

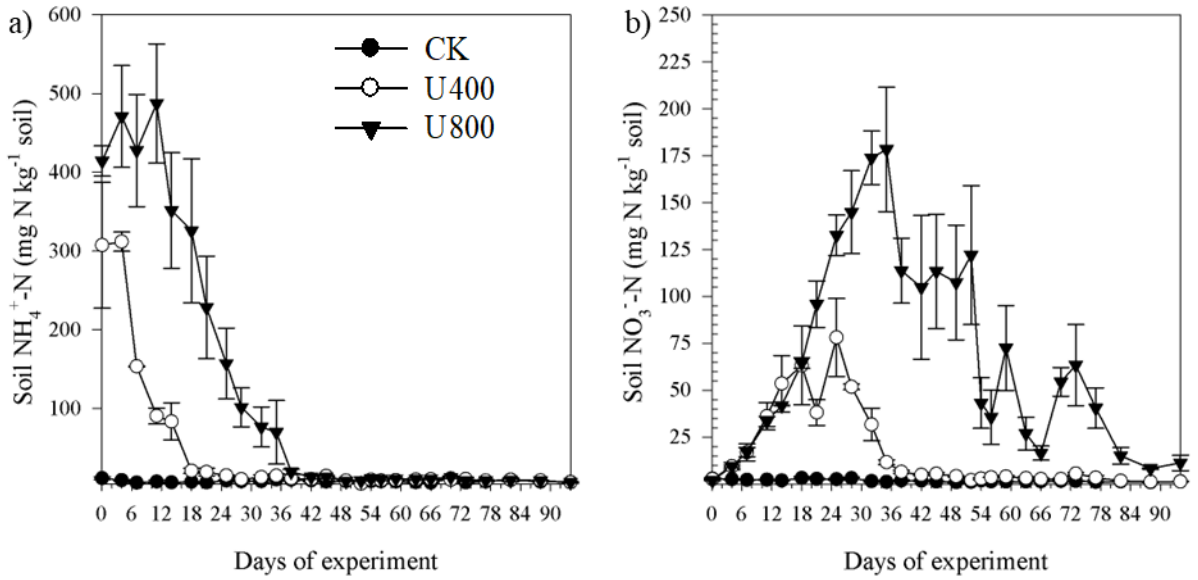

Figure 2. Temporal changes in soil ammonium-N (a) and nitrate-N (b) over timefor the 0-7.5 cm soil depth following urine application at 400 kg N ha^{-1} (U400), 800 kg N ha^{-1} (U800) or with no urine application (CK). Symbols are means of replicates (*n* = 4) with vertical error bars the standard error of the mean.

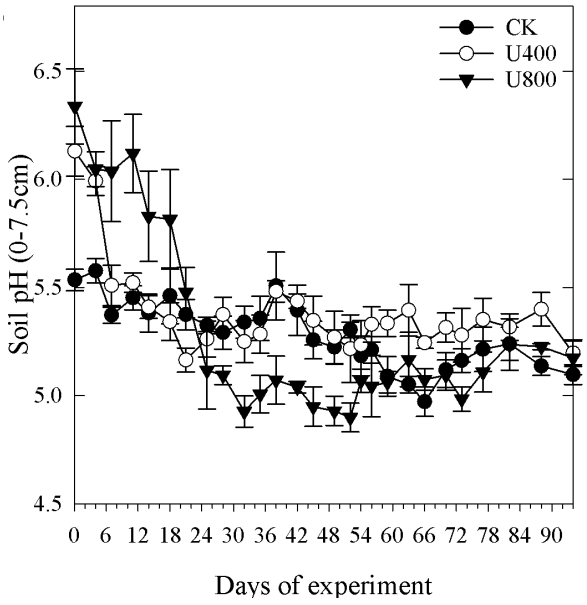

Figure 3. Temporal changes in soil pH over time for the 0-7.5 cm soil depth following urine application at 400 kg N ha^{-1} (U400), 800 kg N ha^{-1} (U800) or with no urine application (CK). Symbols are means of replicates (*n* = 4) with vertical error bars the standard error of the mean.

N_2O and N_2 fluxes

Nitrous oxide fluxes from urine treatments varied temporally and were higher ($P<0.001$) than in the CK treatment until day 51 (Figure 4). The N_2O fluxes increased immediately following urine addition and first peaked on day 7, equal to 0.12 ± 0.13, 4.38 ± 2.05 and 7.71 ± 3.73 mg N m^{-2} day^{-1} in the CK, U400 and U800 treatments, respectively. On day 17, both the U400 and U800 treatments exhibited their highest N_2O fluxes, peaking at 6.95 ± 1.75 and 14.94 ± 3.81 mg N_2O-N m^{-2} day^{-1}, respectively. Averaged over the experimental period the N_2O fluxes from the U800 treatment (2.80 ± 0.33 mg N_2O-N m^{-2} day^{-1}) were higher ($P<0.05$) than from the U400 treatment (1.42 ± 0.16 mg N_2O-N m^{-2} day^{-1}). Over 70% of total N_2O emissions in the U400 and U800 treatments were produced before day 62. The EF_3 value varied with urine rate ($P<0.01$) with values (± SEM) of 0.16 ± 0.08% and 0.43 ± 0.08% for the U400 and U800 treatments, respectively.

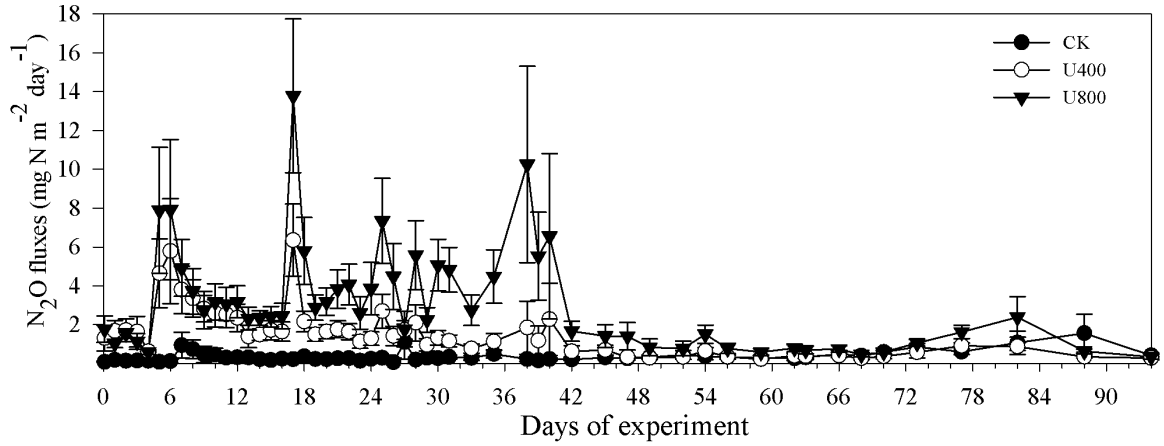

Figure 4. N_2O fluxes over time after urine application with two N loading-rates (U400, 400 kg N ha^{-1} and U800, 800 kg N ha^{-1}) and no urine application (CK). Symbols are means of replicates (*n* = 6) with vertical error bars for the standard error of the mean.

Following urine deposition codenitrification derived N_2 fluxes generally occurred before day 40 (Figure 5a). However, these fluxes were often orders of magnitude lower than denitrification fluxes (Figure 5b). Codenitrification derived N_2 production initially peaked at day 5, but the highest flux occurred later at day 17. Denitrification derived N_2 fluxes generally occurred from day 0 to day 56 (Figure 5b). However, there was no significant difference in the magnitude of the N_2 fluxes due to urine treatment over this period with average denitrification fluxes of 190 ± 27 mg N m^{-2} day^{-1} and 164 ± 26 mg N m^{-2} day^{-1}, in the U400 and U800 treatments, respectively.

For denitrification derived N_2 fluxes, there was a distinct peak immediately after urine deposition at day 0; 399 ± 245 and 668 ± 152 mg N m^{-2} day^{-1} in the U400 and U800 treatments, respectively. Then the denitrification derived N_2 fluxes fluctuated with rainfall in the first month following urine deposition, over the range of 0 to 668 ± 152 mg N m^{-2} day^{-1}. The maximum denitrification derived N_2 flux occurred on day 56 following a period of soil drainage (increasing Dp/Do) with almost no detectable flux after this time.

Cumulative N_2 production via codenitrification equated to 0.48 ± 0.17 and 0.30 ± 0.06 g N m^{-2} in the U400 and U800 treatments, respectively. Cumulative N_2 production as a result of denitrification equalled 12.67 ± 1.62 g N m^{-2} and 11.27 ± 1.60 g N m^{-2} in the U400 and U800 treatments. Consequently, denitrification dominated N_2 production, contributing 97.9 to 98.5% of total N_2 production over the experimental period in the U400 and U800 treatments, respectively.

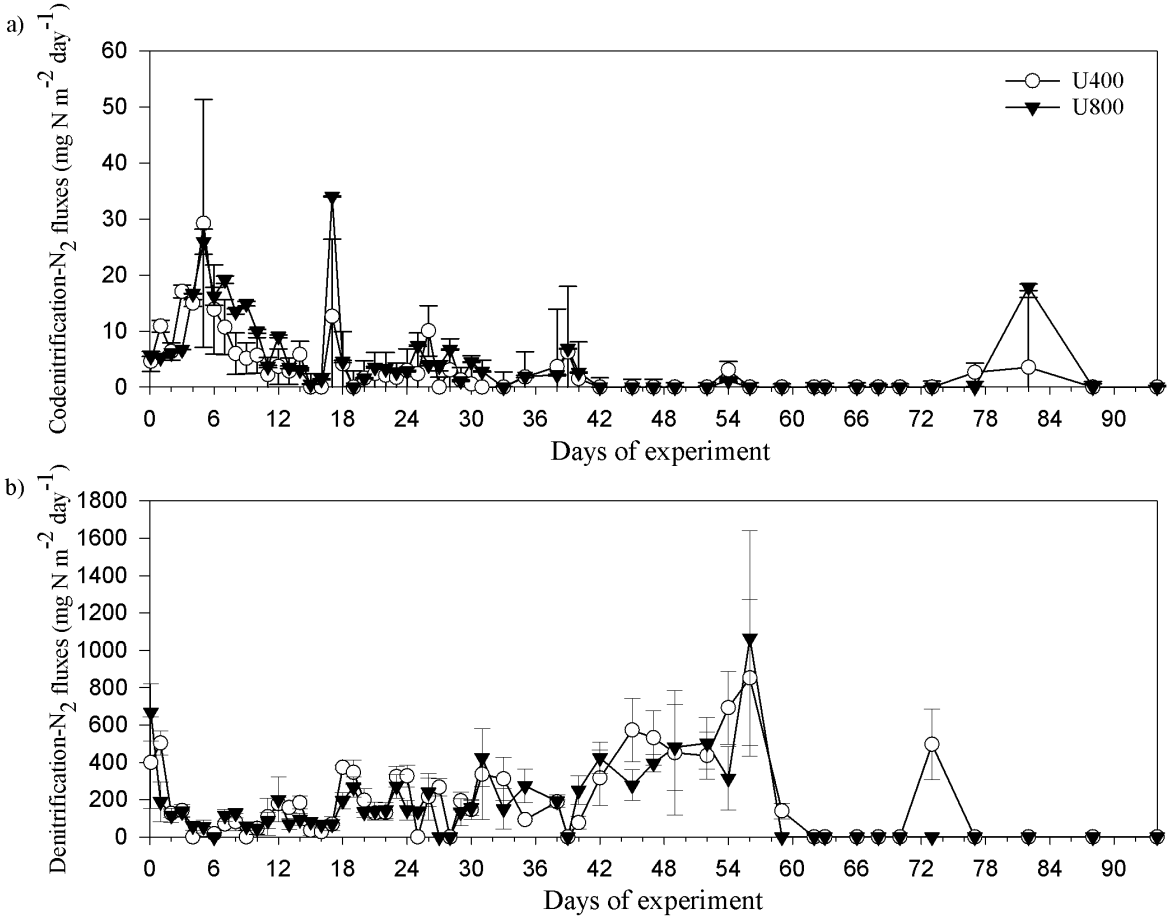

Figure 5. N_2 fluxes from codenitrification (a) and denitrification (b) over time after urine application with two N loading rates (U400, 400 kg N ha^{-1} and U800, 800 kg N ha^{-1}). Symbols are means of replicates (*n* = 6) with vertical error bars for the standard error of the mean. Note different y-axis scales between a) and b).

^{15}N recovery

On day 94 the soil NH_4^+-N concentration did not differ with treatment and declined with increasing soil depth from ~ 6 mg kg^{-1} soil at 0-7.5 cm to ~ 1 mg kg^{-1} soil at 30-45 cm depth (Figure 6a). The soil NO_3^--N concentration at this time did not differ between the CK and U400 treatments but was ~ 3-fold higher in the U800 treatment and declined with soil depth (Figure 6b). Total N in the soil (organic + inorganic) did not vary with treatment, averaging 6336 mg kg^{-1} soil at 0-7.5 cm and declining with soil depth (Figure 6c). On day 94, soil ^{15}N enrichment was higher in both the U400 and U800 treatments when compared with the CK treatment for all soil depths (Figure 6d). There was no difference in the soil ^{15}N enrichment with urine N rate at either 0-7.5 cm or 7.5-15 cm soil depths, however, in the U800 treatment soil ^{15}N enrichment

was higher in the 15-30 cm and 30-45 cm depths than in the U400 treatment (Figure 6d). On day 94 the ^{15}N recovery from soil in the U400 treatment (13.22 ± 0.86%) was higher than that in U800 (8.60 ± 1.06%) for the 0-7.5 cm layer but did no differ for the other depths (Figure 6e). Soil ^{15}N recovery over the 0-45 cm depth, as a percentage of N applied, did not differ with urine treatment and averaged 18.56 ± 0.60 and 16.03 ± 0.52% in the U400 and U800 treatments, respectively.

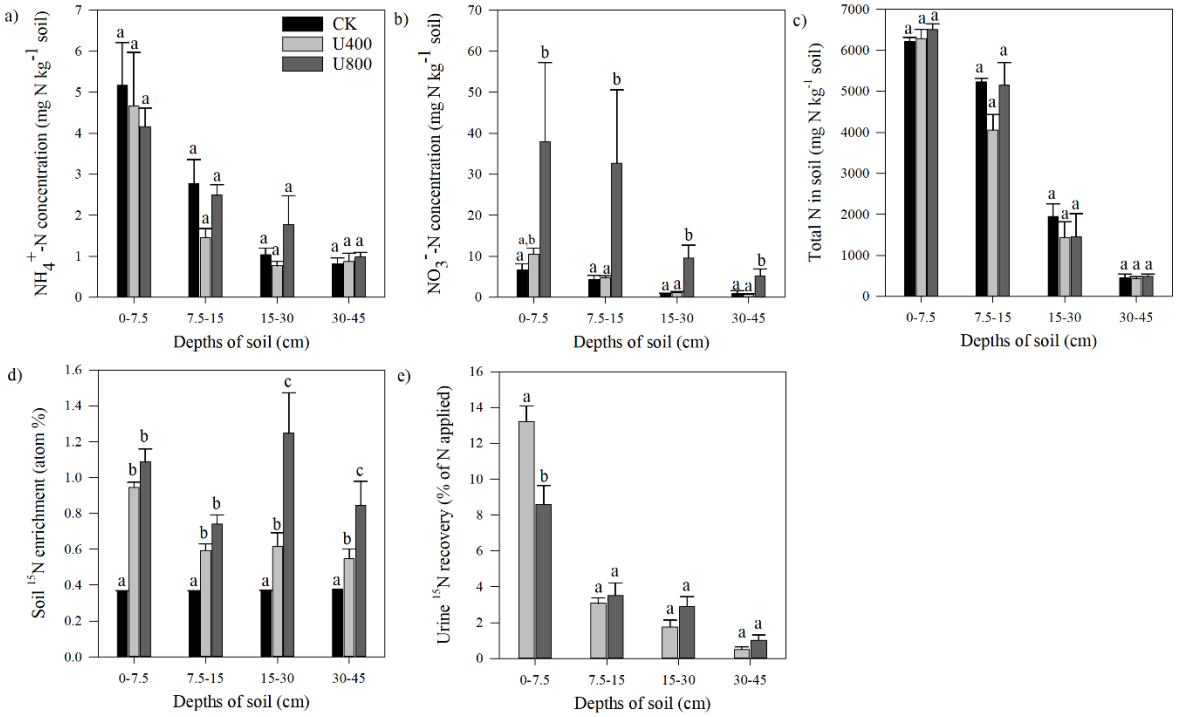

Figure 6. Ammonium-N concentration (a), nitrate-N concentration (b), total N (c), atom % ^{15}N enrichment (d), and urine ^{15}N recovery (e) from 4 different depths (0-7.5 cm, 7.5-15 cm, 15-30 cm, 30-45 cm) soil collected from chambers on day 94, respectively. Symbols are means (*n* = 6) with vertical error bars for the standard error of the mean. Different letters denote significant differences (P<0.05) between treatments.

As a consequence of the lower (P<0.05) ^{15}N recoveries in the soil (0-7.5 cm depth), in pasture, and as N_2, the total ^{15}N recovery was lower in the U800 treatment (40.75 ± 2.17%) compared with the U400 treatment (65.79 ± 4.32%; Table 2).

Table 2. Percentage recovery of ^{15}N after 95 days following urine application at the N loading rate of either 400 (U400) or 800 (U800) kg N ha^{-1}. Values are means (*n* = 6) with errors equal to standard error of the mean.

% of urinary-^{15}N	Soil (0-7.5 cm)	Soil (7.5-15 cm)	Soil (15-30 cm)	Soil (30-45 cm)	Plant	N_2O	N_2 (True)	N_2 (CO)	Total
U400	13.22 ± 0.86^a	3.07 ± 0.31^a	1.76 ± 0.37^a	0.50 ± 0.16^a	14.72 ± 0.51^a	0.35 ± 0.09^a	31.68 ± 4.06^a	0.48 ± 0.18^a	65.79 ± 4.32^a
U800	8.60 ± 1.06^b	3.52 ± 0.71^a	2.90 ± 0.55^a	1.02 ± 0.29^a	9.92 ± 0.75^b	0.41 ± 0.05^b	14.08 ± 2.00^b	0.30 ± 0.07^a	40.75 ± 2.17^b

N_2(True) refers to N_2 production from denitrification pathway and N_2 (CO) refers to N_2 production from codenitrification pathway. Different letters denote significant differences (P<0.05) between treatments.

Discussion

Urine application resulted in soil inorganic-N concentrations typical of those previously reported (Clough et al., 2009). Urease is ubiquitous in soils and it rapidly hydrolyses urea to form NH_4^+, bicarbonate, and hydroxide ions (Jarvis and Pain, 1990). This explains the fast elevation of soil NH_4^+ concentrations following urine application. The peak NH_4^+ concentration in the U800 treatment was not double that observed in the U400 treatment and the maximum NO_3^- concentrations from both treatments did not correspond to observed peak NH_4^+ concentrations, probably due to the different transformation/loss pathways occurring simultaneously. First, the soil NH_4^+ pool following urine deposition does not comprise NH_4^+ sourced solely from the deposited urea: high concentrations of cations in the applied urine form a new equilibrium with NH_4^+ on the soil's cation exchange sites, potentially releasing antecedent NH_4^+ into soil solution (Rex et al., 2021). Second, the formation of hydroxide ions raises the soil pH causing NH_4^+ to be lost from the soil solution as NH_3 due to the elevated soil pH (pH > 7.0) favouring the formation of NH_3 (Sherlock et al., 1994).

The soil NH_4^+ concentrations remained elevated for a period of days prior to decreasing, and longer in the U800 treatment. While the presence of NH_3 can affect nitrifiers this has only been specifically shown for NO_2^- oxidisers in soil (Venterea et al., 2015; Breuillin-Sessoms et al., 2017). Thus, the delay in NH_4^+ oxidation in the current study was most likely due to the time required for the AOB population to respond to the enhanced substrate supply (Di et al., 2009), rather than inhibition of NH_4^+ oxidation. Interestingly, the similar rate of decline in NH_4^+ concentration in both urine treatments in the present study, once nitrification commenced, suggests that the net rate of NH_4^+ oxidation was similar regardless of urine-N application rate. Hence, the time required for the soil NH_4^+ concentration, in the U800 treatment, to reach that of the CK treatment was longer due to the higher initial NH_4^+ load. The relatively low soil NH_4^+ concentrations, at all soil depths on day 94, indicate that nitrification of urine-derived N was complete. The lack of any significant increase in NO_2^- and the similar timing and rates of increase in the NO_3^- concentration between the two urine N rates also demonstrate that NO_2^- oxidisers were not inhibited by NH_3.

Consequently, as hypothesised, the U800 treatment resulted in both higher, and prolonged, soil NO_3^- concentrations in the 0-7.5 cm depth over time. The lack of any difference between the control treatment and the U400 treatment with soil depth of 30-45 cm indicates that the urine induced NO_3^- pool was utilised by plants, immobilised or denitrified by day 94. In contrast, the elevated soil NO_3^- concentrations on day 94, down to soil depth of 45 cm, in the U800 treatment demonstrate the rate of N applied exceeded both plant demands and the capacity for the soil to either immobilise or denitrify the surplus N over this time. Total-N in soil and ^{15}N enrichment values on day 94 reflected the mix of soil organic-N and inorganic-N but were heavily weighted by the natural ^{15}N abundance of the organic-N since inorganic-N on day 94 represented $\leq 1.6\%$ of the soil organic-N pool.

The increased inorganic-N pool under the U800 treatment would induce greater losses of N_2O and N_2, it was almost 2-fold higher average daily flux of N_2O observed in the U800 treatment, and the higher EF_3 value in the U800 treatment than in the U400 treatment. The N_2O EF_3 values were typical of those previously reported (van der Weerden et al., 2011). The additional N_2O flux in the U800 treatment occurred predominately from days 18 to 40 when the NH_4^+ pool was elevated in the U800 treatment, with nitrification of NH_4^+ effectively completed in the U400 treatment, and when the NO_3^- pool was more than 2-fold greater in the U800 treatment. The soil's WFPS and Dp/Do status also indicate the soil was predominately anaerobic or hypoxic from days 18 to 40, and thus the mechanisms for the production of the N_2O at this time

could have been denitrification and/or nitrifier-denitrification. Ammonia oxidising bacteria (AOB) perform nitrifier denitrification under hypoxic conditions, with the process producing N_2O when NO_2^- is reduced via nitric oxide (NO) to form N_2O (Stein, 2019). The AOB can also produce N_2O under anaerobic conditions via the anaerobic oxidation of hydroxylamine by the cytochrome P460 (Stein, 2019). Hence, it is possible that AOB pathways contributed to the N_2O flux over days 18-40. Over this time there was also sufficient NO_3^- and carbon substrate available for denitrification and the higher rate of N_2O production may have been the result of greater denitrification activity, but with denitrification not going to completeness due to factors affecting the $N_2O/(N_2O+N_2)$ ratio. Fluxes of N_2O declined after day 40, primarily because the soil was more aerobic as indicated by trends in Dp/Do.

The higher urinary-N rate, which swamped plant N demand, did not produce higher N_2 fluxes over any period of the measurement. This may have been the result of greater urinary-N inducing NH_3 losses in the U800 treatment. The lack of a soil surface pH measurement in this study prevents estimates of NH_3 emissions (Sherlock et al., 1994; Clough et al., 2018). However, the prolonged elevation of the bulk soil (0-7.5 cm depth) pH in the U800 treatment, until day 18, suggests the soil surface in the U800 treatment may have been conducive (pH > 7) for NH_3 volatilisation over this period. Greater leaching of NO_3^-, as demonstrated by the elevated soil NO_3^- concentrations with increasing soil depth, where reduced C substrate supply and lower denitrifier numbers generally occur, could have also reduced the potential for N_2 production in the U800 treatment. Previously, application of synthetic ^{15}N labelled urine (1000 kg N ha^{-1}) to a Te Kowhai soil resulted in macropore flow below 50 cm depth that resulted in 12% of the urine-N leaching as urea (Clough et al., 1998). If urinary-N was indeed lost via macropore flow in the current study, the resulting reduction in the NO_3^- pool available for denitrification would have been proportional in terms of both the U400 and U800 treatments and cannot explain the lack of any enhanced N_2 flux in the U800 treatment.

While repeated sampling for N_2O accommodates potential gas diffusion gradient effects resulting from the chamber methodology, the single sampling time for N_2 does not. Hence, if the N_2 gas diffusion gradient was disproportionately affected as a result of the higher urine N rate, this may have caused greater underestimation of the N_2 flux in the U800 treatment. Such an effect has been reported to potentially underestimate N_2 emissions by > 30% (Well et al., 2019).

However, the highest N_2 fluxes occurred after day 50 in both the U400 and U800 treatments, despite low NO_3^- concentrations in the U400 treatment, and low atom % ^{15}N enrichments of the NO_3^- pool, if it is assumed that the N_2 evolved from a NO_3^- pool with the same atom % ^{15}N enrichment as the N_2O. Denitrification products may become entrapped within the soil when soil moisture contents are too high to permit diffusion of denitrification products from the soil and it may have taken several days for gas to evolve from the soil surface after being generated under anaerobic conditions (Letey et al., 1980; Clough et al., 2000; Thomas et al., 2019). Such a phenomenon explains why the relatively high N_2 emissions occurred during days 42-56 in both the U400 and U800 treatments. Over this time period, the values of Dp/Do increased. Hence, the functional diffusive pore volume increased as the soil became more aerobic, permitting entrapped N_2 to be emitted following the prolonged period of low Dp/Do and high WFPS, prior to day 42, that would have favoured generation and entrapment of N_2.

In the current study, codenitrification mainly occurred over the first 30 days when soil NH_4^+ concentrations were higher. Codenitrification is a biotic nitrosation process which is favoured under neutral soil pH conditions where an N atom from a nucleophile (e.g. hydroxylamine (NH_2OH) or NH_3,) combines with a N atom from NO_2^- or NO to form hybrid N-N gases (Spott et al., 2011). Both NH_2OH, NO and NO_2^- are intermediaries in the nitrification pathway and

may have contributed to codenitrification, especially during the first 30 days. The relatively small contribution of codenitrification to the total N_2 flux in the current study contrasts with the lysimeter study of Selbie et al. (2015b) where 97% of the N_2 flux was derived from codenitrification following urine deposition. This may be the result of differing soil types, associated microbial communities, higher soil pH, urine-N rates, and rainfall patterns. Selbie et al. (2015b) recorded their results as soil WFPS declined from ca. 90% to ca. 20% WFPS but with regular wetting events as a result of rainfall. This may have facilitated more opportunities for nucleophile generation compared to the current study where the soil Dp/Do values indicate the soil was generally anaerobic over the first 30 days. The higher soil pH in the study of Selbie et al. (2015b) may also have favoured codenitrification due to the more neutral pH condition (Spott et al., 2011). Increased soil NO_2^- concentrations have been reported to enhance codenitrification and in the current study NO_2^- concentrations did not become elevated. However, NO_2^- accumulation has been reported with a urea rate of 1000 kg N ha^{-1} (Venterea et al., 2015) which is the rate used by (Selbie et al., 2015b) and this effect may have contributed to enhanced codenitrification. Other field and laboratory studies have also found limited or nil codenitrification (Clough et al., 2017; Friedl et al., 2017) and further studies are needed to better understand the conditions that generate hybrid N_2 formation via codenitrification *in situ*.

Conclusions

The rate of urinary-N had no effect on daily N_2 fluxes, when soil gas diffusivity indicated soil was suitable for denitrification. Thus, in contrast to N_2O fluxes, N_2 fluxes were not proportional to urine-N rate. Models designed for understanding pasture N balances and dynamics under urinary-N deposition need to consider the pasture's N uptake potential and competition for this with other processes (e.g. NH_3 volatilisation). This determines the magnitude of the ensuing residual N pools that may further contribute to denitrification and other forms of N loss such as leaching. Our results did not align with previously recognised influences on this ratio from controlled laboratory studies, such as the soil NO_3^- concentration, due to the unique and dynamic nature of multiple N pools and processes occurring in the ruminant urine patches of pasture soils. Of note was the apparent release of entrapped N_2 from the soil during periods of drainage. These results also emphasise the difficulty of applying, and the need to improve, the ^{15}N gas flux method over long-term *in situ* studies where soil mineralisation contributes to dilution of soil inorganic ^{15}N pools.

Acknowledgment

The authors would like to acknowledge the technical staff at both AgResearch and Lincoln University for their assistance with this study. This study was funded by the AgResearch Strategic Science Investment Fund and the Lincoln University NZ/China Water Research Centre programme. The results of this study got published on the journal "Science of the Total Environment: Ding, K., Luo, J., Clough, T.J., Ledgard, S., Lindsey, S., Di, H.J., 2022. In situ nitrous oxide and dinitrogen fluxes from a grazed pasture soil following cow urine application at two nitrogen rates. Science of the Total Environment 838, 156473. http://dx.doi.org/10.1016/j.scitotenv.2022.156473

References

Arah, J.R.M., 1997. Apportioning nitrous oxide fluxes between nitrification and denitrification using gas-phase mass spectrometry. Soil Biology and Biochemistry 29, 1295-1299.

Aylward, G.H., Findlay, T.J.V., 1973. SI chemical data. New York, Wiley.

Balaine, N., Clough, T.J., Beare, M.H., Thomas, S.M., Meenken, E.D., 2016. Soil gas diffusivity controls N_2O and N_2 emissions and their ratio. Soil Science Society of America Journal 80, 529-540.

Bates, D., Mächler, M., Bolker, B., Walker, S., 2014. Package "lme4": Linear Mixed-Effects Models using "Eigen" and S4. . R package version 1.1-1.

Blakemore, L., Searle, P., Daly, B., 1987. Methods for chemical analysis of soils. New Zealand Soil Bureau Scientific, Report 80. New Zealand, Lower Hutt: New Zealand Society of Soil Science, p103.

Breuillin-Sessoms, F., Venterea, R.T., Sadowsky, M.J., Coulter, J.A., Clough, T.J., Wang, P., 2017. Nitrification gene ratio and free ammonia explain nitrite and nitrous oxide production in urea-amended soils. Soil Biology and Biochemistry 111, 143-153.

Butterbach-Bahl, K., Baggs, E.M., Dannenmann, M., Kiese, R., Zechmeister-Boltenstern, S., 2013. Nitrous oxide emissions from soils: how well do we understand the processes and their controls? Philosophical Transactions of the Royal Society B: Biological Sciences 368, 20130122.

Clough, T., Jarvis, S., Dixon, E., Stevens, R., Laughlin, R., Hatch, D., 1998. Carbon induced subsoil denitrification of ^{15}N-labelled nitrate in 1 m deep soil columns. Soil Biology and Biochemistry 31, 31-41.

Clough, T., Kelliher, F., Wang, Y., Sherlock, R., 2006. Diffusion of ^{15}N-labelled N_2O into soil columns: a promising method to examine the fate of N_2O in subsoils. Soil Biology and Biochemistry 38, 1462-1468.

Clough, T., Sherlock, R., Cameron, K., 2000. Entrapment and displacement of nitrous oxide in a drained pasture soil. Nutrient cycling in agroecosystems 57, 191-193.

Clough, T., Stevens, R., Laughlin, R., Sherlock, R., Cameron, K., 2001. Transformations of inorganic-N in soil leachate under differing storage conditions. Soil Biology and Biochemistry 33, 1473-1480.

Clough, T.J., Balaine, N., Cameron, K.C., Petersen, S., Sommer, S.G., 2018. Effects of dairy shed effluent dry matter content on ammonia and nitrous oxide emissions from a pasture soil. The Journal of Agricultural Science 156, 1070-1078.

Clough, T.J., Lanigan, G.J., De Klein, C.A., Samad, M.S., Morales, S.E., Rex, D., Bakken, L.R., Johns, C., Condron, L.M., Grant, J., 2017. Influence of soil moisture on codenitrification fluxes from a urea-affected pasture soil. Scientific Reports 7, 1-12.

Clough, T.J., Ray, J.L., Buckthought, L.E., Calder, J., Baird, D., O'Callaghan, M., Sherlock, R.R., Condron, L.M., 2009. The mitigation potential of hippuric acid on N_2O emissions from urine patches: An in situ determination of its effect. Soil Biology and Biochemistry 41, 2222-2229.

de Klein, C.A., Luo, J., Woodward, K.B., Styles, T., Wise, B., Lindsey, S., Cox, N., 2014. The effect of nitrogen concentration in synthetic cattle urine on nitrous oxide emissions. Agriculture, Ecosystems & Environment 188, 85-92.

Di, H.J., Cameron, K.C., Shen, J., Winefield, C.S., O'Callaghan, M., Bowatte, S., He, J., 2009. Nitrification driven by bacteria and not archaea in nitrogen-rich grassland soils. Nature Geoscience 2, 621-624.

Dominati, E.J., Mackay, A.D., Bouma, J., Green, S., 2016. An ecosystems approach to quantify soil performance for multiple outcomes: the future of land evaluation? Soil Science Society of America Journal 80, 438-449.

Friedl, J., Scheer, C., Rowlings, D.W., McIntosh, H.V., Strazzabosco, A., Warner, D.I., Grace, P.R., 2016. Denitrification losses from an intensively managed sub-tropical pasture–Impact of soil moisture on the partitioning of N_2 and N_2O emissions. Soil Biology and Biochemistry 92, 58-66.

Friedl, J., Scheer, C., Rowlings, D.W., Mumford, M.T., Grace, P.R., 2017. The nitrification inhibitor DMPP (3, 4-dimethylpyrazole phosphate) reduces N_2 emissions from intensively managed pastures in subtropical Australia. Soil Biology and Biochemistry 108, 55-64.

Ganasamurthy, S., Rex, D., Samad, M.S., Richards, K.G., Lanigan, G.J., Grelet, G.-A., Clough, T.J., Morales, S.E., 2021. Competition and community succession link N transformation and greenhouse gas emissions in urine patches. Science of the Total Environment 779, 146318.

Hallin, S., Philippot, L., Löffler, F.E., Sanford, R.A., Jones, C.M., 2018. Genomics and ecology of novel N_2O-reducing microorganisms. Trends in Microbiology 26, 43-55.

Haynes, R., Williams, P., 1993. Nutrient cycling and soil fertility in the grazed pasture ecosystem. Advances in agronomy 49, 119-199.

Highton, M.P., Bakken, L.R., Dörsch, P., Wakelin, S., de Klein, C.A.M., Molstad, L., Morales, S.E., 2020. Soil N_2O emission potential falls along a denitrification phenotype gradient linked to differences in microbiome, rainfall and carbon availability. Soil Biology and Biochemistry 150, 108004.

IPCC, 2019. Chapter 11: N_2O emissions from managed soils, and CO_2 emissions from lime and urea application, In: K. Hergoualc'h, H.A., M. Bernoux, N. Chirinda, A. del Prado, Å. Kasimir, J.D. MacDonald, S.M. Ogle, K. Regina, T.J. van der Weerden (Ed.). Intergovernmental Panel on Climate Change (IPCC).

IPCC, 2022. The IPCC Sixth Assessment Report WGIII climate assessment of mitigation pathways: from emissions to global temperatures, In: Kikstra, J.S., Nicholls, Z.R., Smith, C.J., Lewis, J., Lamboll, R.D., Byers, E., Sandstad, M., Meinshausen, M., Gidden, M.J., Rogelj, J. (Eds.), Geoscientific Model Development, pp. 9075-9109.

Jarvis, S., Pain, B., 1990. Ammonia volatilisation from agricultural land, Proceedings.

Jones, D., Willett, V., 2006. Experimental evaluation of methods to quantify dissolved organic nitrogen (DON) and dissolved organic carbon (DOC) in soil. Soil Biology and Biochemistry 38, 991-999.

Khan, S., Clough, T., Goh, K., Sherlock, R., 2011. Influence of soil pH on NOx and N_2O emissions from bovine urine applied to soil columns. New Zealand Journal of Agricultural Research 54, 285-301.

Letey, J., Jury, W., Hadas, A., Valoras, N., 1980. Gas diffusion as a factor in laboratory incubation studies on denitrification. Wiley Online Library.

Luo, D., Ganesh, S., Koolaard, J., 2018. Predictmeans: Calculate predicted means for linear models. R package version 1.0.1.

Luo, J., Ledgard, S., 2020. New Zealand dairy farm systems and key environmental effects. Frontiers of Agricultural Science and Engineering 8, 148-158.

Moldrup, P., Chamindu Deepagoda, T., Hamamoto, S., Komatsu, T., Kawamoto, K., Rolston, D.E., de Jonge, L.W., 2013. Structure‐dependent water‐induced linear reduction model for predicting gas diffusivity and tortuosity in repacked and intact soil. Vadose Zone Journal 12, 1-11.

Morales, S.E., Jha, N., Saggar, S., 2015. Biogeography and biophysicochemical traits link N_2O emissions, N_2O emission potential and microbial communities across New Zealand pasture soils. Soil Biology and Biochemistry 82, 87-98.

Mulvaney, R., 1984. Determination of ^{15}N‐labeled dinitrogen and nitrous oxide with triple‐collector mass spectrometers. Soil Science Society of America Journal 48, 690-692.

Mulvaney, R., Boast, C., 1986. Equations for determination of nitrogen‐15 labeled dinitrogen and nitrous oxide by mass spectrometry. Soil Science Society of America Journal 50, 360-363.

Ravishankara, A.R., Daniel, J.S., Portmann, R.W., 2009. Nitrous oxide (N_2O): The dominant ozone-depleting substance emitted in the 21st century. Science 326, 123-125.

Rex, D., Clough, T.J., Lanigan, G.J., Jansen-Willems, A.B., Condron, L.M., Richards, K.G., Müller, C., 2021. Gross N transformations vary with soil moisture and time following urea deposition to a pasture soil. Geoderma 386, 114904.

Samad, M.S., Bakken, L.R., Nadeem, S., Clough, T.J., de Klein, C.A., Richards, K.G., Lanigan, G.J., Morales, S.E., 2016. High-resolution denitrification kinetics in pasture soils link N_2O emissions to pH, and denitrification to C mineralization. PloS one 11, e0151713.

Selbie, D.R., Buckthought, L.E., Shepherd, M.A., 2015a. The challenge of the urine patch for managing nitrogen in grazed pasture systems. Advances in agronomy 129, 229-292.

Selbie, D.R., Lanigan, G.J., Laughlin, R.J., Di, H.J., Moir, J.L., Cameron, K.C., Clough, T.J., Watson, C.J., Grant, J., Somers, C., 2015b. Confirmation of co-denitrification in grazed grassland. Scientific Reports 5, 1-9.

Shan, J., Sanford, R.A., Chee‐Sanford, J., Ooi, S.K., Löffler, F.E., Konstantinidis, K.T., Yang, W.H., 2021. Beyond denitrification: The role of microbial diversity in controlling nitrous oxide reduction and soil nitrous oxide emissions. Global change biology 27, 2669-2683.

Sherlock, R.R., Freney, J.R., Bacon, P.E., van der Weerden, T.J., 1994. Estimating ammonia volatilization from unsaturated urea fertilized and urine affected soils by an indirect method. Fertilizer research 40, 197-205.

Singh, B.P., Mehra, P., Fang, Y., Dougherty, W., Saggar, S., 2021. Nitrous oxide emissions from cow urine patches in an intensively managed grassland: Influence of nitrogen loading under contrasting soil moisture. Science of the Total Environment 757, 143790.

Spott, O., Russow, R., Stange, C.F., 2011. Formation of hybrid N_2O and hybrid N_2 due to codenitrification: First review of a barely considered process of microbially mediated N-nitrosation. Soil Biology and Biochemistry 43, 1995-2011.

Stein, L.Y., 2019. Insights into the physiology of ammonia-oxidizing microorganisms. Current Opinion in Chemical Biology 49, 9-15.

Stepniewski, W., 1980. Oxygen diffusion and strength as related to soil compaction. 1. ODR (oxygen diffusion rate). Polish Journal of Soil Science 13, 3-13.

Stevens, R., Laughlin, R., 2001. Lowering the detection limit for dinitrogen using the enrichment of nitrous oxide. Soil Biology and Biochemistry 33, 1287-1289.

Stevens, R.J., Laughlin, R.J., Atkins, G.J., Prosser, S.J., 1993. Automated determination of nitrogen-15-labeled dinitrogen and nitrous oxide by mass spectrometry. Soil Science Society of America Journal 57, 981-988.

Thomas, S.M., Fraser, P.M., Hu, W., Clough, T.J., van der Klei, G., Wilson, S., Tregurtha, R., Baird, D., 2019. Tillage, compaction and wetting effects on NO_3, N_2O and N_2 losses. Soil Research 57, 670-688.

van der Weerden, T.J., Luo, J., de Klein, C.A., Hoogendoorn, C.J., Littlejohn, R.P., Rys, G.J., 2011. Disaggregating nitrous oxide emission factors for ruminant urine and dung deposited onto pastoral soils. Agriculture, Ecosystems & Environment 141, 426-436.

Venterea, R.T., Clough, T.J., Coulter, J.A., Breuillin-Sessoms, F., Wang, P., Sadowsky, M.J., 2015. Ammonium sorption and ammonia inhibition of nitrite-oxidizing bacteria explain contrasting soil N_2O production. Scientific Reports 5, 12153.

Well, R., Maier, M., Lewicka-Szczebak, D., Köster, J.R., Ruoss, N., 2019. Underestimation of denitrification rates from field application of the ^{15}N gas flux method and its correction by gas diffusion modelling. Biogeosciences 16, 2233-2246.